On the Canonical Grid Method for Two-Dimensional Scattering Problems

Joel T. Johnson, *Member, IEEE*

Abstract—The banded matrix iterative approach with a canonical grid expansion (BMIA/CAG) has been shown in [1] to be an efficient method for the calculation of scattering for near planar two-dimensional (2-D) geometries such as one-dimensional rough surfaces. However, in [1], only the first three terms in the canonical grid series for TE polarization above a perfectly conducting surface were discussed and methods for implementing only a portion of these terms were presented. In this paper, a general form for all terms in the canonical grid series is provided for both TE and TM polarizations above an impedance surface and an efficient algorithm for calculating their contributions is described. The relationship between the canonical grid and operator expansion methods is also discussed. A sample surface scattering problem is shown to illustrate the utility of higher order terms in the canonical grid method.

Index Terms— Electromagnetic scattering, moment methods, rough surfaces.

I. INTRODUCTION

SEVERAL improved numerical methods [1]–[6] for the calculation of fields scattered by two-dimensional (2-D) geometries have recently been developed which allow computations for structures very large in terms of a wavelength (up to tens of thousands of wavelengths) in reasonable computational times. One of these methods, the banded matrix iterative approach with canonical grid expansion (BMIA/CAG) [1], applies for near planar geometries and is based on a separation of the matrix $\overline{\overline{Z}}$ in a point-matching method of moments formulation into a sum of two matrices $\overline{\overline{Z}}^{(s)} + \overline{\overline{Z}}^{(w)}$ called the strong and weak matrices, respectively. Strong matrix elements are the exact matrix elements of the method of moments formulation up to a specified distance (or bandwidth) from the testing point in each row and zero otherwise resulting in a banded matrix form. Weak matrix terms exist outside the strong matrix bandwidth and are based on a canonical grid expansion of the exact matrix elements into a series of translationally invariant terms times powers of the height differences between points, resulting in a form which can be multiplied using the fast Fourier transform (FFT). This rewritten matrix is then applied in a conjugate gradient solution of the matrix equation $(\overline{\overline{Z}}^{(s)} + \overline{\overline{Z}}^{(w)})\overline{I} = \overline{V}$ with required matrix multiplies performed rapidly due to the banded nature

of the strong matrix and use of the FFT for weak matrix multiplies. Storage limitations for large geometry problems are avoided by recalculating strong matrix elements on each conjugate gradient iteration and by storing only the translationally invariant portions of the canonical grid series. The matrix equation can also be solved by direct banded matrix solution of the strong matrix equation iterated to include weak matrix contributions. Reference [1] discusses both of these solution methods for TE polarized fields above a perfectly conducting surface and presented the first three terms in the canonical grid series. However, for many problems, more terms in the series are required to obtain an accurate result. In this paper, a general form for weak matrix terms for both TE and TM polarizations above an impedance boundary condition surface are presented and an efficient algorithm for implementing their contributions is described. In addition, the relationship between the operator expansion [4] and canonical grid methods is discussed.

II. INTEGRAL EQUATIONS

Fig. 1 illustrates a surface profile $z = f(x)$, which is irregular only in the plane of incidence (taken to be the $x - z$ plane) and constant perpendicular to the plane of incidence (the y direction) for which Maxwell's equations decouple into dual equations for TE and TM waves. Applying a scalar Kirchhoff diffraction integral in terms of E_y for the TE case and H_y for the TM case with the 2-D Hankel function form of the Green's function [7] results in

$$\frac{E_y(\overline{r})}{2} = E_y^{\text{inc}} + \int dS'$$
$$\cdot \left\{ E_y(\overline{r}') \frac{\partial g(\overline{r}, \overline{r}')}{\partial n} - g(\overline{r}, \overline{r}') \frac{\partial E_y(\overline{r}')}{\partial n} \right\} \quad (1)$$

for the TE case with incident field E_y^{inc} and

$$\frac{H_y(\overline{r})}{2} = H_y^{\text{inc}} + \int dS'$$
$$\cdot \left\{ H_y(\overline{r}') \frac{\partial g(\overline{r}, \overline{r}')}{\partial n} - g(\overline{r}, \overline{r}') \frac{\partial H_y(\overline{r}')}{\partial n} \right\} \quad (2)$$

for the TM case with incident field H_y^{inc} where the domain of integration is the surface profile S' in the plane of incidence and a principle value integration is implied. In the above equation

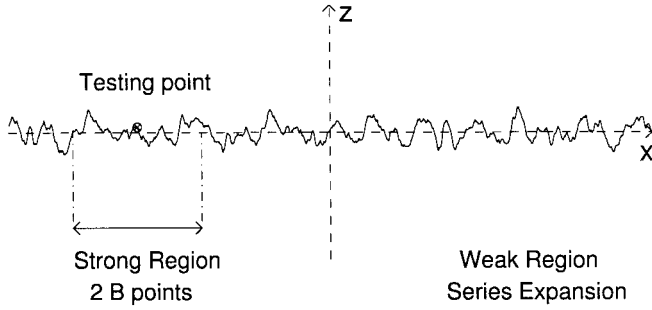$$g(\overline{r}, \overline{r}') = \frac{i}{4} H_0^{(1)}(k|\overline{r} - \overline{r}'|) \quad (3)$$

Fig. 1. Geometry of problem.

where $k = \omega\sqrt{\mu_0 \epsilon_0}$ is the propagation constant in free-space and $H_0^{(1)}$ is the zeroth order Hankel function of the first kind.

The above formulation gives one integral equation in two unknowns (E_y and $\partial E_y/\partial n$ or H_y and $\partial H_y/\partial n$) on the surface profile. Use of the impedance boundary condition [8] on the surface reduces this to one unknown through the relationships

$$E_y = \frac{i}{k}\sqrt{\frac{\epsilon_0}{\epsilon_1}}\left(\frac{\partial E_y}{\partial n}\right) \qquad (4)$$

$$\frac{\partial H_y}{\partial n} = \frac{k}{i}\sqrt{\frac{\epsilon_0}{\epsilon_1}}(H_y) \qquad (5)$$

for TE and TM polarizations, respectively, where ϵ_0 and ϵ_1 are the permittivities of the nonmagnetic regions above and below the surface profile, respectively.

Applying a point-matching method of moments technique [9] results in a matrix equation in terms of the unknown pulse-basis function expansion coefficients of these fields. Elements of the impedance matrix $\overline{\overline{Z}}$ are

$$Z_{mn} = \frac{ik}{4}\Delta x H_1^{(1)}(k\sqrt{(x_m - x_n)^2 + (z_m - z_n)^2})$$
$$\cdot \frac{z_m - z_n - \dfrac{\partial f(x_n)}{\partial x}(x_m - x_n)}{\sqrt{(x_m - x_n)^2 + (z_m - z_n)^2}}$$
$$- \frac{k\Delta x}{4}\sqrt{\frac{\epsilon_0}{\epsilon_1}}H_0^{(1)}$$
$$\cdot (k\sqrt{(x_m - x_n)^2 + (z_m - z_n)^2})$$
$$\cdot \sqrt{1 + \left(\frac{\partial f(x_n)}{\partial x}\right)^2}, \qquad m \neq n \qquad (6)$$

$$Z_{mm} = -\frac{1}{2} - \frac{k\Delta x}{4}\sqrt{\frac{\epsilon_0}{\epsilon_1}}\left\{1 + \frac{2i}{\pi}\left(\log\left[\frac{k\Delta x}{4e}\right.\right.\right.$$
$$\left.\left.\left.\cdot \sqrt{1 + \left(\frac{\partial f(x_n)}{\partial x}\right)^2}\right] + \gamma\right)\right\}$$
$$\cdot \sqrt{1 + \left(\frac{\partial f(x_n)}{\partial x}\right)^2} \qquad (7)$$

for the TM case and

$$Z_{nm} = -\frac{1}{4}\sqrt{\frac{\epsilon_0}{\epsilon_1}}\Delta x H_1^{(1)}(k\sqrt{(x_m - x_n)^2 + (z_m - z_n)^2})$$
$$\cdot \frac{z_m - z_n - \dfrac{\partial f(x_n)}{\partial x}(x_m - x_n)}{\sqrt{(x_m - x_n)^2 + (z_m - z_n)^2}}$$
$$+ \frac{i\Delta x}{4}H_0^{(1)}(k\sqrt{(x_m - x_n)^2 + (z_m - z_n)^2})$$
$$\cdot \sqrt{1 + \left(\frac{\partial f(x_n)}{\partial x}\right)^2}, \qquad m \neq n \qquad (8)$$

$$Z_{mm} = -\frac{i}{2k}\sqrt{\frac{\epsilon_0}{\epsilon_1}} + \frac{i\Delta x}{4}\left\{1 + \frac{2i}{\pi}\left(\log\left[\frac{k\Delta x}{4e}\right.\right.\right.$$
$$\left.\left.\left.\cdot \sqrt{1 + \left(\frac{\partial f(x_n)}{\partial x}\right)^2}\right] + \gamma\right)\right\}$$
$$\cdot \sqrt{1 + \left(\frac{\partial f(x_n)}{\partial x}\right)^2} \qquad (9)$$

for TE, assuming a single point approximation of basis function integrals. In the above equations, γ represents the Euler number 0.577216, m refers to the surface point index of the testing point n the integration point where $x_m = m\Delta x$, $x_n = n\Delta x$, and $\partial f(x_n)/\partial x$ refers to the surface profile derivative evaluated at the point $x = x_n$. Note that tables of the zero and first order Hankel functions can be stored in the computer code implemented to avoid multiple calls to Hankel routines as strong matrix terms are regenerated on each conjugate gradient iteration.

III. Canonical Grid Expansion

As mentioned previously, strong matrix elements contain the exact terms (6) and (7) or (8) and (9) up to a specified distance from the matrix diagonal. Outside this distance, weak matrix elements are expanded in the canonical grid series by expressing the Hankel functions as

$$H_0^{(1)}(k\sqrt{(x_m - x_n)^2 + (z_m - z_n)^2})$$
$$= \sum_{j=0}^{\infty}\frac{H_j^{(1)}(k|x_m - x_n|)}{j!}\left[\frac{-k(z_m - z_n)^2}{2|x_m - x_n|}\right]^j \qquad (10)$$

$$H_1^{(1)}(k\sqrt{(x_m - x_n)^2 + (z_m - z_n)^2}$$
$$= \sum_{j=0}^{\infty}\frac{H_{j+1}^{(1)}(k|x_m - x_n|)}{j!|x_m - x_n|}\left[\frac{-k(z_m - z_n)^2}{2|x_m - x_n|}\right]^j \qquad (11)$$

which can be derived either using a power series expansion about $z_m - z_n = 0$ or through the Bessel function product

theorem [10]. Reference [1] provided the first three terms in (10); the above equations describe all terms and allow some insight into convergence properties. Note that [10] gives a condition of validity of this expansion as $|z_m - z_n| < |x_m - x_n|$, indicating that strong matrix bandwidths should be chosen in most cases to provide a larger strong interaction region than maximum peak-to-peak surface heights. An additional criterion that allows further insight is obtained by observing in the far field where $H_j^{(1)}$ may be approximated by $(-i)^j H_0^{(1)}$ to provide

$$
H_0^{(1)}(k\sqrt{(x_m - x_n)^2 + (z_m - z_n)^2}
$$
$$
\approx H_0^{(1)}(k|x_m - x_n|) \sum_{j=0}^{\infty} \frac{1}{j!} \left[\frac{ik(z_m - z_n)^2}{2|x_m - x_n|} \right]^j \quad (12)
$$

$$
\approx H_0^{(1)}(k|x_m - x_n|) \exp\left[\frac{ik(z_m - z_n)^2}{2|x_m - x_n|} \right] \quad (13)
$$

$$
\frac{H_1^{(1)}(k\sqrt{(x_m - x_n)^2 + (z_m - z_n)^2}}{\sqrt{(x_m - x_n)^2 + (z_m - z_n)^2}}
$$
$$
\approx \frac{H_1^{(1)}(k|x_m - x_n|)}{|x_m - x_n|} \sum_{j=0}^{\infty} \frac{1}{j!} \left[\frac{ik(z_m - z_n)^2}{2|x_m - x_n|} \right]^j \quad (14)
$$

$$
\approx \frac{H_1^{(1)}(k|x_m - x_n|}{|x_m - x_n|} \exp\left[\frac{ik(z_m - z_n)^2}{2|x_m - x_n|} \right]. \quad (15)
$$

Thus, in the far field, the canonical grid expansion essentially provides a power series expansion of the Fresnel phase term of the Green's function. Since numerical use of this approach requires truncation of this power series in a finite number of terms, only surfaces with small maximum values of $k(z_m - z_n)^2 / 2|x_m - x_n|$ are suitable for this method. The author has used up to 15 terms in the canonical grid series for surfaces with maximum values of $k(z_m - z_n)^2 / 2|x_m - x_n|$ of up to 4.0, but the well-known poor convergence of an exponential power series expansion for larger arguments makes the approach impractical. It is interesting to note that the convergence parameter involves the product of height separation relative to wavelength $k|z_m - z_n|$ and slope of the line joining points (x_n, z_n) and (x_m, z_m), $|z_m - z_n|/|x_m - x_n|$ terms for $|x_m - x_n|$ outside the strong matrix distance. Thus, the approach is applicable for surfaces with large heights relative to a wavelength as long as these "chordal" slopes remain sufficiently small, which can be insured by increasing the strong matrix region (bandwidth). However, for large rms height surfaces the bandwidth required can become impractical in smaller problems. For example, the approach was not successful for propagation predictions over hilly terrain in [11] due to large terrain height variations (more than 100λ) even though terrain slopes were small everywhere. However, such large height variations are not expected over the ocean surface at frequencies 1 GHz or lower. The author currently uses a second code to assess the maximum value of the $k(z_m - z_n)^2 / 2|x_m - x_n|$ parameter for a given surface and

strong matrix bandwidth before deciding how many canonical grid series terms to use based on the exponential power series expansion. Although these calculations are order N^2 compared to the order $N \log N$ BMIA/CAG code, a greatly reduced number of surface profile points can be used to assess this parameter for surfaces whose main height contributions come from longer spatial frequency components of the spectrum, such as the ocean surface. Tests varying the strong matrix bandwidth can be used to determine the relationship between this bandwidth and the number of CAG series terms required for a given surface profile to optimize computational times. These tests are only intended to serve as guidelines since they are derived from a far-field expansion. The canonical grid expansion in the near field could require additional terms depending on the strong matrix bandwidth used and surface height statistics, although no significant effects were observed by the author in the sample case to be discussed in Section VI.

IV. IMPLEMENTATION

Applying the canonical grid expansion to weak matrix elements results in

$$
Z_{mn} = \frac{ik}{4} \Delta x \left\{ z_m - z_n - \frac{\partial f(x_n)}{\partial x} (x_m - x_n) \right\}
$$
$$
\cdot \sum_{j=0}^{\infty} \frac{H_{j+1}^{(1)}(k|x_m - x_n|)}{j! |x_m - x_n|} \left[\frac{-k}{2|x_m - x_n|} \right]^j
$$
$$
\cdot (z_m - z_n)^{2j} - \frac{k\Delta x}{4} \sqrt{\frac{\epsilon_0}{\epsilon_1}} \sqrt{1 + \left(\frac{\partial f(x_n)}{\partial x} \right)^2}
$$
$$
\cdot \sum_{j=0}^{\infty} \frac{H_j^{(1)}(k|x_m - x_n|)}{j!} \left[\frac{-k}{2|x_m - x_n|} \right]^j
$$
$$
\cdot (z_m - z_n)^{2j} \quad (16)
$$

for TM polarization (TE is very similar and will no longer be separately addressed), recognizable as a combination of two series of terms, which are primarily functions of $x_m - x_n$ times powers of $(z_m - z_n)$. Expanding these binomial terms into polynomials in z_m and z_n allows use of the FFT to perform canonical grid multiplies since the terms become translationally invariant after pre- and postmultiplication. The procedure is implemented by initially generating all translationally invariant terms in the series (i.e., the functions only of $x_m - x_n$) and Fourier transforming them before beginning the conjugate gradient solution. Then, at each weak matrix multiplication required in the conjugate gradient iterations, for each canonical grid series term, the vector to be multiplied by the matrix is first multiplied by the appropriate power of z_n in the polynomial (and by $\sqrt{1 + (\partial f(x_n)/\partial x)^2}$ or $\partial f(x_n)/\partial x$ if necessary) and Fourier transformed as well. Convolution is performed by multiplying the two Fourier transformed vectors and inverse transforming them to obtain the matrix vector product and appropriate powers of z_m from the binomial expansion are then post-multiplied in the spatial domain.

As an example, consider the matrix elements (16) using two terms in the canonical grid series (a maximum j value in (16)

$$Z_{mn} = \frac{ik}{4}\,\Delta x \left\{ z_m - z_n - \frac{\partial f(x_n)}{\partial x}\,(x_m - x_n) \right\}$$

$$\cdot \left[\frac{H_1^{(1)}(k|x_m - x_n|)}{|x_m - x_n|} - \frac{kH_2^{(1)}(k|x_m - x_n|}{2|x_m - x_n|^2} \right.$$

$$\cdot (z_m - z_n)^2 \bigg] - \frac{k\Delta x}{4}\sqrt{\frac{\epsilon_0}{\epsilon_1}}\sqrt{1 + \left(\frac{\partial f(x_n)}{\partial x}\right)^2}$$

$$\left[H_0^{(1)}(k|x_m - x_n|) - \frac{kH_1^{(1)}(k|x_m - x_n|)}{2|x_m - x_n|} \right.$$

$$\cdot (z_m - z_n)^2 \bigg] \tag{17}$$

which can be rewritten as (18), as shown at the bottom of the page.

Expression (18) contains fourteen terms involving powers of $z_m = f(x_m)$ or $z_n = f(x_n)$; all of these $\alpha = 1$ to 14 terms can be written in the form

$$Z_{mn}^\alpha = h_\alpha[x_m - x_n]u_\alpha[x_m]v_\alpha[x_n] \tag{19}$$

where $h_\alpha[\cdot], u_\alpha[\cdot]$ and $v_\alpha[\cdot]$ are appropriate functions corresponding to each of the fourteen terms. The multiplication of these terms times a vector $\overline{I}$ can be written as

$$w_m^\alpha = \sum_{l=0}^N Z_{ml}^\alpha\,I_l \tag{20}$$

$$= \sum_{l=0}^N u_\alpha[m\Delta x]\,h_\alpha[(m-l)\Delta x]v_\alpha[l\Delta x]\,I_l \tag{21}$$

$$= u_\alpha[m\Delta x]\sum_{l=0}^N h_\alpha[(m-l)\Delta x]\,V_l \tag{22}$$

where $V_l = v_\alpha[l\Delta x]\,I_l$. The convolutional nature of this multiplication is now evident after vector $\overline{V}$ is generated by pre-multiplication of the elements of $\overline{I}$ by v_α. The sum over l is performed for all values of m simultaneously using the FFT, resulting in the observed increased efficiency and the u_α functions of m only are incorporated by post-multiplication after the FFT step. Finally, a sum over α includes all terms in the complete weak matrix multiplication. Refer to [1] for a more detailed discussion of the three-term case.

For each canonical grid series term in the TM impedance boundary case, three translationally invariant vectors are actually required to be stored corresponding to the $(H_j^{(1)}(k|x_m - x_n|)/[-k/2|x_m - x_n|]^j)$, $(H_{j+1}^{(1)}(k|x_m - x_n|)/j!|x_m - x_n|)[-k/2|x_m - x_n|]^j$, and $-(x_m - x_n)(H_{j+1}^{(1)}(k|x_m - x_n|)/j!|x_m - x_n|)[-k/2|x_m - x_n|]^j$ portions of the matrix elements, as is evident from (18). These three terms are used in four separate convolution steps for each canonical grid term since the $(H_{j+1}^{(1)}(k|x_m - x_n|)/j!|x_m - x_n|)[-k/2|x_m - x_n|]^j$ term must be pre-multiplied by z_n in one of these operations and postmultiplied in the other to generate the $z_m - z_n$ term in $\{z_m - z_n - (\partial f(x_n)/\partial x)(x_m - x_n)\}$.

The number of FFT operations required in a canonical grid series multiplication goes as $4(M^2 + 4M + 2)$ for $j_{max} = M$ terms in the expansion due to the increasing number of polynomial terms in the expansion of $(z_m - z_n)^{2j}$. This assumes reuse of Fourier transformed z_n premultiplied terms as in the following pseudocode algorithm.

For an array I to be multiplied,

```
do k_1 = 0, 2M
    k_3 = 1, N
    do k_3 = 1, N
        f(k_3) = I(k_3) * z(k_3)^{k_1}
    enddo
    do k_3 = N + 1, 2N
        f(k_3) = 0
    enddo
    ff = FFT(f)
    do k_2 = int[(k_1 - 1)/2] + 1, M
        do k_3 = 1, 2N
            g(k_3) = ff(k_3) * h(k_3, k_2)
        enddo
        gg = IFFT(g)
        do k_3 = 1, N
            c(k_3) = c(k_3) + gg(k_3 + N - 1)
                * z(k_3)^{(2k_2 - k_1)} * \binom{2k_2}{k_1}
        enddo
    enddo
enddo
```

where M refers to the number of canonical grid series terms, N to the number of unknowns in the matrix equation, the FFT and IFFT operators refer to the fast Fourier transform and its inverse, respectively, of size $2N$, z refers to an array containing the surface profile heights, c refers to an array containing the result of the matrix multiplication for

$$Z_{mn} = \frac{ik}{4}\Delta x \left[\frac{H_1^{(1)}(k|x_m - x_n|)}{|x_m - x_n|}\,(z_m - z_n) - \frac{kH_2^{(1)}(k|x_m - x_n|)}{2|x_m - x_n|^2}\,(z_m^3 - 3z_m^2 z_n + 3z_m z_n^2 - z_n^3) \right]$$

$$- \frac{\partial f(x_n)}{\partial x}\,\frac{ik}{4}\Delta x \left[\frac{H_1^{(1)}(k|x_m - x_n|)}{|x_m - x_n|} - \frac{kH_2^{(1)}(k|x_m - x_n|)}{2|x_m - x_n|^2}\,(z_m^2 - 2z_m z_n + z_n^2) \right](x_m - x_n)$$

$$- \frac{k\Delta x}{4}\sqrt{\frac{\epsilon_0}{\epsilon_1}}\sqrt{1 + \left(\frac{\partial f(x_n)}{\partial x}\right)^2}\left[H_0^{(1)}(k|x_m - x_n|) - \frac{kH_1^{(1)}(k|x_m - x_n|}{2|x_m - x_n|}\,(z_m^2 - 2z_m z_n + z_n^2) \right]. \tag{18}$$

the specified portion of the matrix element, and $\binom{2k_2}{k_1}$ is the binomial coefficient which results from the polynomial expansion of the $(z_m - z_n)^{2j}$ terms. $h(k_3, k_2)$ in the above pseudocode refers to the Fourier transformed canonical grid series term of size $2N$ corresponding to $j = k_2$ with k_3 the index of the FFT result. Note that the int operation is intended to truncate decimal portions of real numbers into integers with the exception that for $k_1 = 0$ the loop over k_2 is intended to be from zero to M to include all z_n^0 terms; some languages may interpret the integer operations defining this loop differently. For the impedance boundary condition case, four of these loops are needed to include the varying portions of the exact matrix elements with their individual contributions added to obtain the complete weak matrix multiplication. The rapidly increasing number of FFT operations required as M increases again shows that the CAG approach becomes impractical for large values of M, usually due to larger rms height surfaces. However, the overall method remains order $N \log N$ so that even for large rms height surfaces, it will be more efficient than an order N^2 technique for large values of N. For smaller rms height surfaces with small values of M, the canonical grid method should be an extremely efficient order $N \log N$ method.

V. RELATIONSHIP WITH OPERATOR EXPANSION METHOD (OEM)

A second recently proposed efficient technique for rough surface scattering involves use of an expansion of the normal derivative operator in the integral equations into a series of operations involving the FFT [4]. For perfectly conducting surfaces, use of this series allows direct computation of induced currents on the surface to a given order in the operator expansion series from the incident field. The same set of operations can be obtained through consideration of the canonical grid method with zero strong matrix bandwidth. Consider the TE perfectly conducting surface case in which only the $j = 0$ canonical grid term is retained. In this case, matrix elements are proportional to the second line of (16) and using only the $j = 0$ term in the series results in a single convolutional operation required for the matrix multiply. Thus, the matrix equation can be solved in the Fourier domain by taking the FFT of the right-hand side, dividing by the Fourier transform of the convolutional kernel and inverse transforming to obtain the spatial domain induced currents, as described in [4]. Higher order operator expansion results can be obtained by retaining more terms in the canonical grid series and by expanding induced currents into a perturbation series with $k(z_m - z_n)^2/2|x_m - x_n|$ serving as the small parameter. Higher order approximations to the induced currents then follow as additional FFT operations on the previous order approximation. Note that this procedure implements the symmetric operator expansion derived in [4] and yields a straightforward procedure for finding arbitrary order terms in the operator expansion series (only up to third order terms have been considered in [12]).

Since the operator expansion method (OEM) essentially provides an analytical solution (in terms of FFT operations on the incident field) to the canonical grid matrix equation with
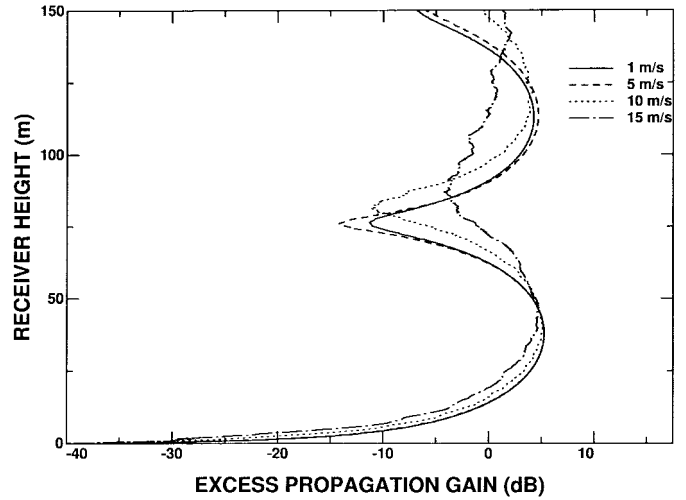

Fig. 2. Excess propagation gain versus receiver height for a 1-GHz horizontal magnetic dipole source 10 m above one realization of a Pierson–Moskowitz ocean surface. Range is 4.92 km.

zero strong bandwidth and truncated in a finite number of CAG series terms, the OEM has the same limitations as the canonical grid approach and, in fact, is more limited due to the absence of a strong matrix region. However, for surfaces for which the $k(z_m - z_n)^2/2|x_m - x_n|$ product is small enough between all pairs of points, the OEM provides a more efficient solution of the matrix equation since no conjugate gradient solvers are required. Use of a strong matrix region in the canonical grid method prevents the analytical solution of the OEM from being obtained, but avoids use of the CAG expansion near the testing point where it is most likely to be inaccurate. A combination of the two methods can be used to provide a more efficient solution, with the operator expansion method used as a preconditioner for the canonical grid conjugate gradient solution. This approach has been applied for perfectly conducting surfaces and found to yield greatly improved convergence, but as yet has not been implemented for the impedance surfaces considered in this paper.

VI. SAMPLE RESULTS

Application of the BMIA/CAG method to ocean propagation under a standard atmosphere enables rough surface effects on propagation to be observed. Fig. 2 illustrates received power relative to that in free-space for a horizontal magnetic dipole receiver (TM case) as a function of receiver height. A 1.0-GHz horizontal magnetic dipole source is located 10 m above the ocean surface 4.92 km ($16\,384\ \lambda$) away, with the four points per wavelength sampling rate found sufficient for propagation problems in [11] resulting in 65 536 unknowns. Earth curvature and atmospheric effects are included by fitting the ocean surface profile to a sphere with radius 4/3 that of the earth, which introduces an earth "bulge" of only 35.6 cm so that propagation is essentially line of sight. The ocean surface used is one realization of a Gaussian random process described by a Pierson–Moskowitz spectrum as in [13] and the transmitter and receiver are located at each end of the surface profile as described in [11]. A dielectric constant of

TABLE I
NUMERICAL SIMULATION PARAMETERS FOR $16\,384\ \lambda$ ($65\,536$ UNKNOWNS) CASE

$U_{19.5}$	$k\sigma$	Strong bandwidth (points)	CAG series terms (M)	CG iterations	CPU time
1 m/s	0.113	8	3	1	51 mins
5 m/s	2.82	8	8	1	78 mins
10 m/s	11.3	256	15	2	245 mins
15 m/s	25.4	1024	15	4	548 mins

$76.4 + i65.1$ from the model of [14] is used for sea water, corresponding to a temperature of 10 °C and salinity of 30 parts per thousand (ppt). The four curves of Fig. 2 illustrate propagation over a single surface realization at $U_{19.5}$ wind speeds of 1, 5, 10, and 15 m/s, with k times rms height ($k\sigma$) values of 0.113, 2.83, 11.3, and 25.4, respectively, and show that surface roughness can have significant effects on L-band line of sight propagation. Although a detailed Monte Carlo simulation would be required to determine statistical properties of these effects, the results presented are sufficient to show that surface roughness can introduce variations in ocean propagation for a given realization.

Table I lists the numerical parameters used to run these cases, note the varying strong matrix bandwidths required to allow use of 15 CAG terms as surface roughness increases with windspeed. For these simulations, strong and weak matrix terms were used simultaneously in the conjugate gradient solution as described previously with a second conjugate gradient solution with strong matrix bandwidth zero and only the $j = 0$ CAG series term (whose solution would be given by the operator expansion method for impedance surfaces) used to precondition the iterations. Computational times presented believed to be near optimal, but the range of parameters that can be varied in the BMIA/CAG method, especially at the lower wind speeds, makes this difficult to insure. Codes were run on a Silicon Graphics R5000 workstation with computational times for each case and the number of conjugate gradient (CG) iterations required listed in the table as well. Simulations for a $32\,768\ \lambda$ terrain profile case in [11] without the canonical grid expansion required approximately one week CPU time, corresponding to around two days for the $16\,384$ λ surfaces of this case. Use of the CAG series is observed to significantly reduce this time, even in cases where a large number of CAG series terms are required.

VII. CONCLUSIONS

Complete canonical grid series terms in the BMIA/CAG approach to scattering from one-dimensional rough impedance surfaces were described. An efficient algorithm for implementing the multiplication of a matrix containing these terms times a vector was also presented and the method applied to prediction of L-band propagation over single ocean surface realizations for representative wind speeds. Results showed that surface roughness can introduce significant propagation variations in the line of sight for nonducting conditions. The relationship between the canonical grid and operator expansion methods was also considered and the operator expansion solution was shown to be derivable as a solution

of the canonical grid matrix equation with zero strong matrix bandwidth, illustrating that the operator expansion method should be expected to yield no better performance than the canonical grid approach. Further studies of propagation over the ocean made possible through use of the BMIA/CAG approach will continue.

REFERENCES

[1] L. Tsang, C. H. Chan, K. Pak, and H. Sangani, "Monte Carlo simulations of large scale problems of random rough surface scattering and applications to grazing incidence with the BMIA/canonical grid method," *IEEE Trans. Antennas Propagat.*, vol. 43, pp. 851–859, 1995.
[2] D. A. Kapp and G. S. Brown, "A new numerical method for rough surface scattering calculations," *IEEE Trans. Antennas Propagat.*, vol. 44, pp. 711–721, 1996.
[3] D. Holliday, L. L. Deraad, and G. J. St-Cyr, "Forward–backward: A new method for computing low grazing angle scattering," *IEEE Trans. Antennas Propagat.*, vol. 44, pp. 722–729, 1996.
[4] D. M. Milder, "An improved formalism for wave scattering from rough surfaces," *J. Acoust. Soc. Amer.*, vol. 89, pp. 529–541, 1991.
[5] N. Engheta, W. D. Murphy, V. Rokhlin, and M. S. Vassiliou, "The fast multipole method for electromagnetic scattering problems," *IEEE Trans. Antennas Propagat.*, vol. 40, pp. 634–641, 1992.
[6] E. Bleszynski, M. Bleszynski, and T. Jaroszewicz, "A fast integral equation solver for electromagnetic scattering problems," in *IEEE APS/URSI Symp. Conf. Proc.*, 1994, pp. 416–419.
[7] J. A. Kong, *Electromagnetic Wave Theory*, 2nd ed. New York: Wiley, 1990.
[8] K. M. Mitzner, "An integral equation approach to scattering from a body of finite conductivity," *Radio Sci.*, vol. 2, pp. 1459–1470, 1967.
[9] R. F. Harrington, *Field Computation by Moment Methods*. New York: Macmillan, 1968.
[10] I. S. Gradshteyn and I. M. Ryzhik, *Table of Integrals, Series, and Products*, 5th ed., A. Jeffrey, Ed. San Diego, CA: Academic, 1994.
[11] J. T. Johnson, R. T. Shin, J. Eidson, L. Tsang, and J. A. Kong, "A method of moments model for VHF propagation," *IEEE Trans. Antennas Propagat.*, vol. 45, pp. 115–125, 1997.
[12] P. J. Kaczkowski and E. I. Thorsos, "Application of the operator expansion method to scattering from one-dimensional moderately rough Dirichlet random surfaces," *J. Acoust. Soc. Amer.*, vol. 96, pp. 957–966, 1994.
[13] E. I. Thorsos, "Acoustic scattering from Pierson-Moskowitz sea surfaces," *J. Acoust. Soc. Amer.*, vol. 88, pp. 335–349, 1990.
[14] L. A. Klein and C. T. Swift, "An improved model for the dielectric constant of sea water at microwave frequencies," *IEEE Trans. Antennas Propagat.*, vol. 25, pp. 104–111, 1977.

Joel T. Johnson (M'96) received the B.E.E. degree from the Georgia Institute of Technology, Atlanta, in 1991, and the S.M. and Ph.D. degrees from the Massachusetts Institute of Technology, Cambridge, in 1993 and 1996, respectively.

He is currently an Assistant Professor in the Department of Electrical Engineering and ElectroScience Laboratory of The Ohio State University, Columbus. His research interests are in the areas of microwave remote sensing, propagation, and electromagnetic wave theory.

Dr. Johnson is a member of Tau Beta Pi, Eta Kappa Nu, and Phi Kappa Phi. He held a National Science Foundation Graduate Fellowship from 1991 to 1995. He received the 1993 Best Paper Award from the IEEE Geoscience and Remote Sensing Society and the 1997 Office of Naval Research Young Investigator, National Science Foundation CAREER, and PECASE Awards.